Collapse and Stability of Necklace Beams in Kerr Media

Taylor D. Grow, Amiel A. Ishaaya, Luat T. Vuong, and Alexander L. Gaeta*

School of Applied and Engineering Physics, Cornell University, Ithaca, New York 14853, USA

(Received 5 October 2006; published 28 September 2007)

We investigate the spatial dynamics of optical necklace beams in Kerr media. For powers corresponding to less than the critical power for self-focusing per bead, we experimentally confirm the confinement of these necklace beams as proposed in [Phys. Rev. Lett. **81**, 4851 (1998)]. At higher powers, we observe a transition from collective necklace behavior to one in which the beads of the necklace collapse independently. We observe that, below the transition power, the perturbed necklace still behaves in a collective manner with coupling between individual beads but that, at higher powers, it undergoes a similar transition to a decoupled state of the necklace.

DOI: 10.1103/PhysRevLett.99.133902 PACS numbers: 42.65.Jx, 42.65.Tg

The nonlinear Schrödinger equation (NLSE) is used to describe phenomena in many areas of physics including optics [1], plasmas [2], and Bose-Einstein condensates [3]. The 1-D NLSE admits stable exact solutions known as solitons, which in optical systems can be observed in the temporal domain in fibers or in the spatial domain in slab waveguides [4]. In these systems, the nonlinear focusing exactly balances the diffraction in the spatial domain or dispersion in the time domain. For the 2-D NLSE, which describes an optical beam propagating through a bulk Kerr medium, there are no such stable solitonic solutions. For powers above a certain critical power P_{cr}, the beam will self-focus and undergo collapse until higher-order processes such as plasma generation halt the collapse [5], while beams below the P_{cr} will diffract. Spatial 2-D solitons do exist in photorefractive media where the nonlinearity is saturable [4]. The collapse dynamics of beams with different input profiles yields many interesting results and has been studied for Gaussian [6], astigmatic Gaussian [7,8], super-Gaussian [9], and optical vortex [10] input profiles. In each case, the beams are unstable and eventually collapse towards one or more individual Townes profiles [11], which each contain a power equal to P_{cr}.

Necklace beams were first conceived [12] as a spatial profile that would be relatively stable to collapse and could maintain its shape over long propagation distances and thus overcome the spatial instability associated with the 2-D NLSE. Such a beam was first envisioned by taking a string of one-dimensional antiphase solitons and wrapping them into a ring. Each bead approximates a one-dimensional soliton in the radial direction, and by employing the well-known out-of-phase repulsion exhibited by all solitons [4], each bead repels its neighbors in the azimuthal direction. Numerical simulations showed that the individual beads of the necklace remained confined over many diffraction lengths in contrast to the diffraction of a single bead [12–14]. Many other types of rings of beams, similar to necklace beams, have recently been suggested including vector solitons [15], soliton clusters [16], necklacelike solitons in photonic lattices [17], two-color soliton clusters, which exist in media with cubic and quadratic nonlinearities [18,19], and also necklacelike beams in media with cubic and quintic nonlinearities [20]. Nearly all of these studies have been theoretical, and there has been little experimental work verifying such beams. Preliminary experiments made qualitative observations of the confinement of necklacelike beams in a bulk nonlinear medium [21], but the confinement, collapse dynamics, and stability of the beams were not investigated. Rotschild *et al.* [22] have also recently observed necklace beams in highly nonlocal nonlinear media.

In this Letter, we present the first experimental investigation of the collapse dynamics and stability of necklace beams in a Kerr medium. We measure the confinement properties and examine the stability and collapse of the necklace beams at high powers. At intermediate power ranges, when the whole beam power is less than the product of the number of beads and P_{cr}, the beads are coupled together and, if significantly perturbed, will coalesce into one beam and collapse. At higher powers, when each bead has more than one P_{cr} of a Gaussian, the beads collapse independently.

In the original theoretical work [12] on necklace beams, the input profile to the nonlinear medium is $\mathrm{sech}[(r - L)/w]\cos(\omega\theta)$, where r is the transverse radial coordinate, L is the width of the ring of beads, w is the width of each bead, and the diffraction length is $2\pi n w^2/\lambda$. Since such a profile cannot be readily produced experimentally, a natural choice for realizing the beams are the well-known Laguerre-Gaussian (LG) $\mathrm{TEM}_{\rho l}$ modes, which have a necklace shape. With this input, we compare the diffraction of the necklace beam against the diffraction length of the corresponding LG beam, rather than the diffraction length of a single bead, since we believe this provides a more practical measure of confinement of the necklace beam. For example, even in the linear regime, a ring of Gaussians will diffract more slowly than an isolated Gaussian beam.

To model the dynamics of the necklace beams, we use the (2 + 1)-D NLSE, which can be expressed in dimensionless form as

$$i\psi_\zeta + \frac{1}{4}\nabla_\perp^2\psi + \frac{L_{\rm df}}{L_{\rm nl}}|\psi|^2\psi = 0, \quad (1)$$

where $\psi(\nu, \mu, \zeta) = A(x, y, z)/A_0$, A is the amplitude of the envelope of the electric field, A_0 is the peak input amplitude, $\zeta = z/L_{\rm df}$, $\mu = x/r_0$, $\nu = y/r_0$, $\nabla_\perp^2$ is the transverse Laplacian, $L_{\rm df} = kr_0^2/2$, $L_{\rm df}$ is the diffraction length, $L_{\rm nl}$ is the nonlinear length, r_0 is the characteristic radius of the input beam, $k = 2\pi n_0/\lambda$ is the wave number, λ is the vacuum wavelength, n_0 is the linear index of refraction, and n_2 is the nonlinear index coefficient. The last term of the left-hand side gives rise to self-focusing arising from the intensity-dependent refractive index $n = n_0 + n_2 I$. The critical power for self-focusing depends on the input beam profile. In this Letter, $P_{\rm cr}$ denotes the critical power for self-focusing of an isolated Gaussian profile [5].

The experimental setup is shown in Fig. 1. A 90-fs, 800-nm pulse from a Ti:sapphire amplifier is sent through a spatial filter and then passes through a phase plate. The phase plate is a fused-silica substrate in which alternating azimuthal sections are produced using reactive-ion etching. The beam is then passed through a second spatial filter to eliminate the higher-order modes, which leaves the lowest-order LG beam. The beam is then recollimated and sent through different lengths of BK7 glass. In order to probe different ranges of power and avoid plasma formation due to the high intensities, we took data with multiple input diameters and two different lengths of glass. We record the input profile by removing the glass and imaging it onto a 12-bit CCD camera. We then replace the glass and image the output face. In order to observe the collapse dynamics of the beams, we increase the power until just below the threshold of supercontinuum generation, which is a signature of collapse [23].

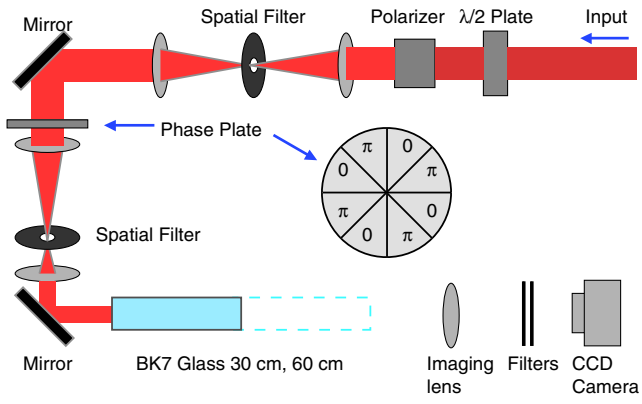

FIG. 1 (color online). Experimental setup for studying propagation of necklace beams. A phase plate with azimuthally alternating phase sections is used to produce the initial necklace profile.

For a 90-fs pulse traveling through such long (30 and 58 cm) lengths of BK7, dispersive effects are not negligible. As the pulse propagates, it broadens, and the peak power decreases. Our simulations do not include the temporal dynamics and thus cannot take into account this change in the peak power. Nevertheless, when comparing the numerical predictions to the experiments, we find that the spatial dynamics and collapse distances are in excellent agreement up to a scaling factor in the input power.

Initially, we investigate the spatial confinement and formation of the necklace beam from the input LG beam. Figure 2 shows the experimental pictures of the confinement of the necklace beam compared with numerical simulations. Figure 2(a) shows the input profile after the second spatial filter. Figure 2(b) shows the beam at the output of 58 cm of glass at low powers (linear diffraction). As the power is increased, the beads of the beam change their shape and draw towards the center, forming a necklace beam as shown in Fig. 2(c). Each individual lobe of the LG forms a circular bead, and the confinement of the total necklace improves as the power is increased. Figure 2(c) is just below the supercontinuum threshold.

The corresponding numerical results are presented in Figs. 2(d)–2(f). The formation of a necklace beam reduces the effects of diffraction as compared to the linear regime, but we find that the profile does not remain truly confined even at distances as short as $4L_{\rm df}$ for a necklace beam with 8 beads. This result is a clarification of the original theoretical claim that necklace beams remained confined over tens of diffraction lengths [12]. By comparing against the diffraction length of a LG beam, which closely approximates a necklace beam, rather than the diffraction length of a single Gaussian, which only approximates an individual lobe, we present an accurate measure of the confinement possible for a necklace beam in the nonlinear regime. The necklace beams are not true solitons since diffraction

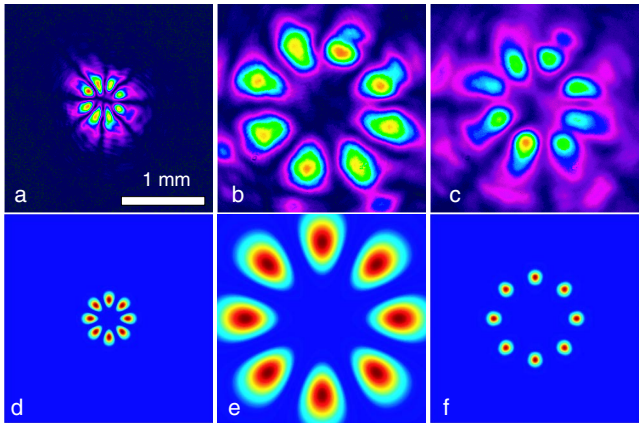

FIG. 2 (color online). Experimentally measured (a)–(c) and simulations (d)–(f) for necklace beams in glass. (a) Input Laguerre-Gaussian, (b) ($E = 1.0$ μJ) after 58 cm of glass, (c) ($E = 7.7$ μJ) after 58 cm of glass. (d) Input Laguerre-Gaussian, (e) low power (i.e., linear diffraction), $\zeta = 4L_{\rm df}$, (f) $P = 8P_{\rm cr}$ at $\zeta = 4L_{\rm df}$.

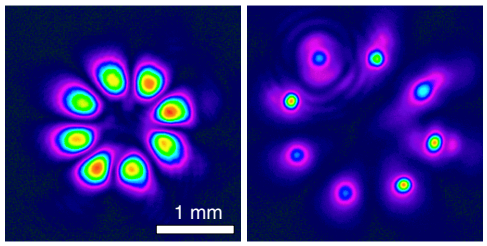

FIG. 3 (color online). Experimentally measured necklace profile at high input pulse energy ($E = 12.2\ \mu$J) (left) at the input and after 30 cm of propagation through glass (right).

effects are still present, albeit at a highly reduced level [12]. However, we find that the necklace beam is unusually stable to azimuthal modulational instability in comparison with other beams in the self-focusing regime such as vortex and ring-shaped profiles, which are unstable and break apart into increasing numbers of filaments as the power is increased; the necklace maintains the same number of beads. Our numerical simulations also show that, even at high powers and with up to 20% amplitude and phase noise, the necklace beams do not break apart or filament as it propagates.

We attempted to dramatically increase the power and observed a corresponding increase in the confinement. We expanded the input profile to avoid supercontinuum generation and used the 30-cm piece of glass. Figure 3 shows the input LG beam at more than twice the energy as in Fig. 2. At higher powers, the beads do not form a necklace beam, but they each collapse to Townes profiles similarly to the behavior of an isolated Gaussian [6]. From the numerical simulations, we find that this transition occurs when the input profile has more than one P_{cr} per bead. Further increases in the power do not change the dynamics but simply hasten the collapse.

Numerical simulations predict that the confinement of the necklace beam improves as the number of beads increases. We attempted to study necklace beams with 16 and 32 beads. However, as the power for a necklace beam is approximately one P_{cr} per bead, in order to avoid high intensities and higher-order effects in the glass, the size of the input profile must be increased. Beams large enough to avoid such high intensities did not undergo sufficient diffraction in our longest sample length (58 cm) to observe any significant confinement. In other physical situations, it might be possible to achieve better confinement.

In order to investigate the stability of necklace beams for the case of severe perturbation, we blocked one lobe of the LG at the input face of the glass. Figure 4 shows the dynamics of a necklace with one blocked bead for an energy of 4.9 μJ. Figure 4(a) is the input, and Fig. 4(b) shows the beam diffracting linearly through 58 cm of glass. Figure 4(c) shows the profile of the beam just before supercontinuum generation, which shows that the initially blocked bead becomes much more intense than the other beads. Identical behavior is observed in the simulations

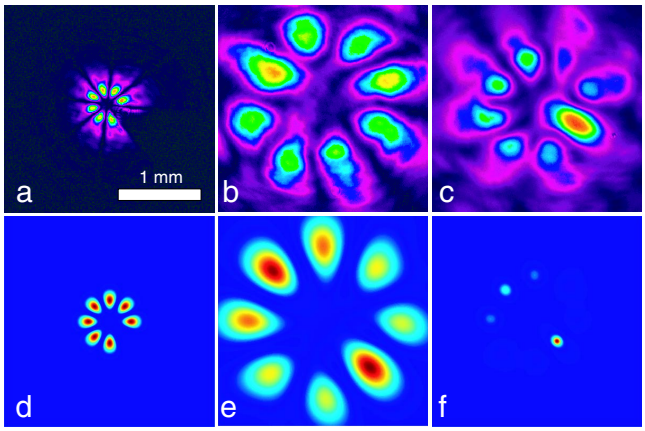

FIG. 4 (color online). Experimentally measured (a)–(c) and simulations (d)–(f) of necklace beam propagation in which the beam is perturbed by removing one of the beads. (a) Input, (b) ($E = 0.7\ \mu$J) after 58 cm of glass, (c) ($E = 4.9\ \mu$J) after 58 cm of glass. (d) Input, (e) linear diffraction for $\zeta = 2.8L_{\mathrm{df}}$, (f) $P = 6P_{\mathrm{cr}}$ at $\zeta = 2.8L_{\mathrm{df}}$.

[Figs. 4(d)–4(f)] for powers at $6P_{\mathrm{cr}}$. We see that, in the regime of linear diffraction, the originally blocked beam reforms with slightly higher intensity than its neighbors. In the nonlinear regime, each bead of the necklace is coupled to its neighbors as it propagates, and one bead eventually collapses on its own. The simulations also show that, even though the total power of the beam is $6P_{\mathrm{cr}}$ in the original beam, only one of the beads collapses.

At higher powers, we observe a transition from this collective behavior. Figure 5 shows the predicted and observed dynamics of a necklace with one blocked bead for $E = 8.4\ \mu$J. Figure 5(a) is the input, and Fig. 5(b) shows the profile of the beam just before supercontinuum occurs. Each of the beams collapses independently of its neighbors into a Townes profile, which is confirmed in the

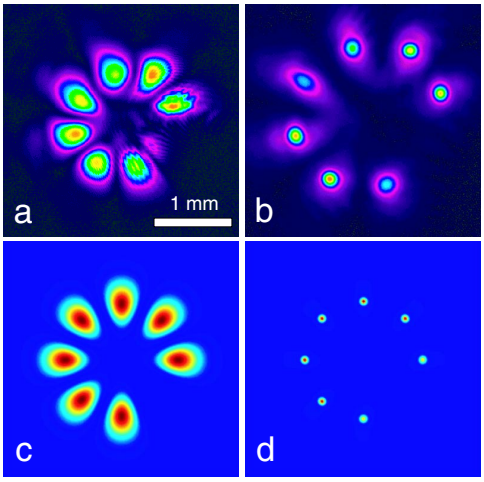

FIG. 5 (color online). Experimentally measured (a),(b) and simulations (c),(d) for a perturbed necklace beam at high power. (a) Input, (b) ($E = 8.4\ \mu$J) after 30 cm of glass, (c) input, (d) $P = 8P_{\mathrm{cr}}$ at $\zeta = 0.2L_{\mathrm{df}}$.

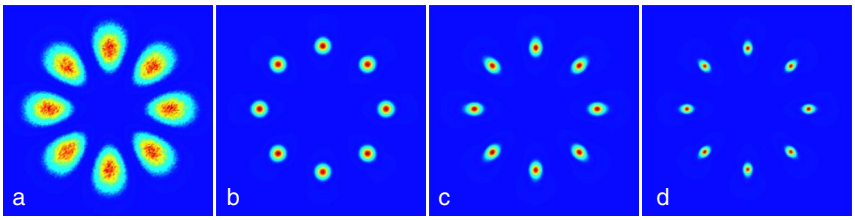

FIG. 6 (color online). Numerical predictions of the collapsing profile for a Laguerre-Gaussian input (a) with 25% amplitude and phase noise for three different powers. (b) $P = 10P_{cr}$ at $\zeta = 0.25L_{df}$, (c) $P = 15P_{cr}$ at $\zeta = 0.15L_{df}$, (d) $P = 20P_{cr}$ at $\zeta = 0.125L_{df}$.

simulations [Figs. 5(c) and 5(d)] for powers at $8P_{cr}$. The abrupt change in the dynamics is also evident in the sharp drop in the distance to collapse from $2.8L_{df}$ in Fig. 4(f) to $0.2L_{df}$ in Fig. 5(d) when the power is increased from 6 to $8P_{cr}$.

Further examination of the numerical simulations shows that the transition for the LG beam with one lobe blocked is rather steep as the power is increased. At $6P_{cr}$ this beam collapses into one bead, and above $7P_{cr}$ each lobe collapses independently into 7 collapse points. The number of collapse points increases linearly with the power in between these two extremes. The beads of the beams are coupled and exchange energy during the propagation in a complicated manner. As soon as any bead has more than one P_{cr}, it will collapse independent of its neighbors.

This results in unique collapse dynamics at high powers when compared to other ring-shaped beams. In the presence of noise, vortex [10] and super-Gaussian beams [9] break apart into individual Townes profiles that increase in number as the power increases. Figure 6 shows the collapse profile for a necklace beam with $10P_{cr}$ [Fig. 6(b)], $15P_{cr}$ [Fig. 6(c)], and $20P_{cr}$ [Fig. 6(d)], which all collapse with the same initial necklace shape. The necklace-shaped collapse pattern is also maintained even with amplitude and phase noise as high as 50%. Thus, the use of LG beams offers a technique for sending arbitrarily large powers in a single beam through a Kerr medium and avoiding self-focusing collapse by shaping the beam into a LG beam with more lobes than there are P_{cr} in the beam.

In conclusion, we have experimentally detailed the confinement of a necklace beam when compared with its linear counterpart LG beam. We have observed appreciable confinement over a few diffraction lengths as compared with the diffraction length of the input LG. Increasing the power resulted in a transition of dynamics from collective necklace behavior to individual collapse of the beads. We also observed that a perturbed necklace beam experiences collective dynamics and collapses to a single bead at intermediate power ranges. At powers above one P_{cr} per bead, we observe that the beads decouple from their neighbors, and each bead catastrophically collapses towards the Townes profile for both the nonperturbed and the perturbed necklace profile. For beams consisting of a combination of out-of-phase Gaussian beams, we expect similar distinct regions of nonlinear behavior.

It is interesting to note that a similar transition between collective and independent dynamics has been observed in semiconductor resonators [24,25]. An initial hexagonal field pattern was formed at low power, exhibiting coherence between the individual lobes which diminished as the nonlinearity was increased. The similarity in the observed transition may indicate a possible general decoupling phenomenon which could be observable in other systems with a Kerr-type nonlinearity.

This work is supported by the National Science Foundation under Grant No. PHY-0244995 and the Army Research Office under Grant No. 48223-PH.

*a.gaeta@cornell.edu

[1] P. L. Kelley, Phys. Rev. Lett. **15**, 1005 (1965).
[2] P. A. Robinson, Rev. Mod. Phys. **69**, 507 (1997).
[3] C. A. Sackett, J. M. Gerton, M. Welling, and R. G. Hulet, Phys. Rev. Lett. **82**, 876 (1999).
[4] G. I. Stegeman and M. Segev, Science **286**, 1518 (1999).
[5] G. Fibich and A. L. Gaeta, Opt. Lett. **25**, 335 (2000).
[6] K. D. Moll, A. L. Gaeta, and G. Fibich, Phys. Rev. Lett. **90**, 203902 (2003).
[7] A. Dubietis, G. Tamosauskas, G. Fibich, and B. Ilan, Opt. Lett. **29**, 1126 (2004).
[8] T. D. Grow and A. L. Gaeta, Opt. Express **13**, 4594 (2005).
[9] T. D. Grow *et al.*, Opt. Express **14**, 5468 (2006).
[10] L. T. Vuong *et al.*, Phys. Rev. Lett. **96**, 133901 (2006).
[11] R. Y. Chiao *et al.*, Phys. Rev. Lett. **13**, 479 (1964).
[12] M. Soljačić, S. Sears, and M. Segev, Phys. Rev. Lett. **81**, 4851 (1998).
[13] M. Soljačić and M. Segev, Phys. Rev. E **62**, 2810 (2000).
[14] M. Soljačić and M. Segev, Phys. Rev. Lett. **86**, 420 (2001).
[15] A. S. Desyatnikov and Y. S. Kivshar, Phys. Rev. Lett. **87**, 033901 (2001).
[16] A. S. Desyatnikov and Y. S. Kivshar, Phys. Rev. Lett. **88**, 053901 (2002).
[17] J. Yang *et al.*, Phys. Rev. Lett. **94**, 113902 (2005).
[18] Y. V. Kartashov, L. C. Crasovan, D. Mihalache, and L. Torner, Phys. Rev. Lett. **89**, 273902 (2002).
[19] D. Mihalache *et al.*, Phys. Rev. E **66**, 016613 (2002); D. Mihalache, D. Mazilu, B. A. Malomed, and F. Lederer, Phys. Rev. E **69**, 066614 (2004).
[20] D. Mihalache *et al.*, Phys. Rev. E **68**, 046612 (2003).
[21] A. Barthelemy *et al.*, Proc. Soc. Photo-Opt. Instrum. Eng. **2041**, 104 (1993).
[22] C. Rotschild *et al.*, Opt. Lett. **31**, 3312 (2006).
[23] A. L. Gaeta, Phys. Rev. Lett. **84**, 3582 (2000).
[24] V. B. Tarenenko, C. O. Weiss, and B. Schäpers, Phys. Rev. A **65**, 013812 (2001).
[25] C. O. Weiss and Y. Larionova, Rep. Prog. Phys. **70**, 255 (2007).